Reply to "Comment on 'Effects of shear methods on shear strengths and deformation modes of two typical transition metal carbides and their unification'"

Chuanying Li,[1] Tao Fu,[1,2,*] Xule Li,[1] Hao Hu,[1] and Xianghe Peng[1,2,†]
[1]*Department of Engineering Mechanics, Chongqing University, Chongqing 400044, China*
[2]*State Key Laboratory of Coal Mine Disaster Dynamics and Control, Chongqing University, Chongqing 400044, China*

(Received 29 September 2023; accepted 20 November 2023; published 5 December 2023)

In our recent study [Phys. Rev. B **107**, 224106 (2023)], we investigated the effects of shear methods on the shear strengths and deformation modes of two typical transition metal carbides using first-principles calculations and preliminarily unified the shear stresses obtained in different ways based on the Mohr-Coulomb relation. Mázdziarz raised a comment on our study and claimed that our work contains some serious and fundamental flaws in the field of continuum mechanics and nanomechanics. Unfortunately, the author seemed to misunderstand our work. Therefore, we respond to the preceding Comment [Phys. Rev. B **108**, 216101 (2023)] on our article to clarify the confusion and misunderstanding.

DOI: 10.1103/PhysRevB.108.216102

First, we would like to sincerely express our gratitude for Mázdziarz's interest in our work [1]. However, after carefully reading the preceding Comment [2], we know that the author may have misunderstood some of our article. To address the issues raised, we provide additional details to clarify the confusion and misunderstanding.

The author stated in the abstract, "The results presented appear to be qualitatively and quantitatively incorrect; they would be correct if we were in the small/linear deformation/strain regime, which we are not. A correct description therefore requires a finite/nonlinear deformation/strain apparatus." It is known that there are two conventional analytical theories to determine the theoretical strength [3], the mean-field theory (such as the Frenkel model), and the finite deformation theory (such as the work by Li and co-workers [3,4]). Wang and Li [4] presented an analytical solution for pure shear in metallic glasses based on finite deformation theory. In addition, there is another modern approach that utilizes the first-principles calculations to obtain the theoretical strength, which is an atomic-scale approach that relies on numerical modeling rather than analytical theories. Our work followed the latter (first-principles calculation) to directly obtain the mechanical response of an atomic system, where the fundamental assumptions used for a continuum may no longer hold true. Although it was suggested that the Cauchy-Born rule could be used to estimate the strain in the system, there is not sufficient evidence showing that the conventional theory for nonlinear and finite deformation can well describe the response of an atomic system without any problems or errors. The purpose of using the Cauchy-Born-rule–based analysis method in our work was to establish a connection between our analysis and continuum mechanics so that readers can more intuitively understand the relevant results.

We will respond one by one to the issues raised in the preceding Comment.

Regarding the left or right multiplication of $\mathbf{F}$ in Eq. (1) of the Comment, we acknowledge that in continuum mechanics, left multiplication is used conventionally. However, in our article [1], the term $\left[\mathbf{I}+\begin{pmatrix}0&0&0\\0&0&0\\0&\Delta\varepsilon_{zy}&0\end{pmatrix}\right]$ is not the deformation gradient $\mathbf{F}$ but the transpose of $\mathbf{F}$; therefore, there is nothing wrong with right multiplication. The detailed derivation process is as follows.

For our incremental loading approach of simple shear, the deformation field is

$$x = X, \quad y = Y + Z\tan\theta, \quad z = Z. \tag{1}$$

We define shear strain

$$\gamma = \tan\theta = \frac{y-Y}{Z} = \frac{\Delta y}{Z} = \frac{\sum_{i=0}^{N}\Delta y_i}{Z} = \sum_{i=0}^{N}\frac{\Delta y_i}{Z} = \sum_{i=0}^{N}\Delta\gamma_i. \tag{2}$$

The schematic is shown in Fig. 1, consistent with the deformation mode illustrated in Fig. 1(a) of our original article [1]. When $i=0$, $\Delta\gamma_0 = 0$, indicating that the deformation has not yet occurred.

According to the Eqs. (1) and (2), we can get

$$\mathbf{F} = \begin{bmatrix}1&0&0\\0&1&\gamma\\0&0&1\end{bmatrix} = \begin{bmatrix}1&0&0\\0&1&\sum_{i=0}^{N}\Delta\gamma_i\\0&0&1\end{bmatrix}. \tag{3}$$

We assume that $\mathbf{F}_n = \begin{bmatrix}1&0&0\\0&1&\sum_{i=0}^{n}\Delta\gamma_i\\0&0&1\end{bmatrix}$. Then the incremental loading approach is adopted as follows: When $n=0$ and $\Delta\gamma_0 = 0$,

$$\mathbf{F} = \mathbf{F}_0 = \mathbf{F}(\Delta\gamma_0) = \begin{bmatrix}1&0&0\\0&1&\Delta\gamma_0\\0&0&1\end{bmatrix} = \begin{bmatrix}1&0&0\\0&1&0\\0&0&1\end{bmatrix} \tag{4}$$

*Corresponding author: futao@cqu.edu.cn
†Corresponding author: xhpeng@cqu.edu.cn

when $n = 1$,

$$\mathbf{F} = \mathbf{F}_1 = \mathbf{F}(\Delta\gamma_1)\cdot\mathbf{F}_0 = \begin{bmatrix} 1 & 0 & 0 \\ 0 & 1 & \Delta\gamma_1 \\ 0 & 0 & 1 \end{bmatrix}\begin{bmatrix} 1 & 0 & 0 \\ 0 & 1 & 0 \\ 0 & 0 & 1 \end{bmatrix} = \begin{bmatrix} 1 & 0 & 0 \\ 0 & 1 & \Delta\gamma_1 \\ 0 & 0 & 1 \end{bmatrix}; \tag{5}$$

when $n = 2$,

$$\mathbf{F} = \mathbf{F}_2 = \mathbf{F}(\Delta\gamma_2)\cdot\mathbf{F}_1 = \begin{bmatrix} 1 & 0 & 0 \\ 0 & 1 & \Delta\gamma_2 \\ 0 & 0 & 1 \end{bmatrix}\begin{bmatrix} 1 & 0 & 0 \\ 0 & 1 & \Delta\gamma_1 \\ 0 & 0 & 1 \end{bmatrix} = \begin{bmatrix} 1 & 0 & 0 \\ 0 & 1 & \Delta\gamma_2 + \Delta\gamma_1 \\ 0 & 0 & 1 \end{bmatrix}; \tag{6}$$

and when $n = N$,

$$\mathbf{F} = \mathbf{F}_N = \mathbf{F}(\Delta\gamma_N)\cdot\mathbf{F}_{N-1} = \begin{bmatrix} 1 & 0 & 0 \\ 0 & 1 & \Delta\gamma_N \\ 0 & 0 & 1 \end{bmatrix}\begin{bmatrix} 1 & 0 & 0 \\ 0 & 1 & \sum_{i=0}^{N-1}\Delta\gamma_i \\ 0 & 0 & 1 \end{bmatrix} = \begin{bmatrix} 1 & 0 & 0 \\ 0 & 1 & \sum_{i=0}^{N}\Delta\gamma_i \\ 0 & 0 & 1 \end{bmatrix} = \begin{bmatrix} 1 & 0 & 0 \\ 0 & 1 & \gamma \\ 0 & 0 & 1 \end{bmatrix}. \tag{7}$$

From Eqs. (4)–(7) we can get

$$\mathbf{F} = \mathbf{F}_N = \mathbf{F}(\Delta\gamma_N)\cdots\mathbf{F}(\Delta\gamma_2)\cdot\mathbf{F}(\Delta\gamma_1)\cdot\mathbf{F}(\Delta\gamma_0). \tag{8}$$

The transpose of Eq. (8) is

$$\mathbf{F}^{\mathrm{T}} = \mathbf{F}_N^{\mathrm{T}} = \mathbf{F}^{\mathrm{T}}(\Delta\gamma_0)\cdot\mathbf{F}^{\mathrm{T}}(\Delta\gamma_1)\cdots\mathbf{F}^{\mathrm{T}}(\Delta\gamma_N) = \begin{bmatrix} 1 & 0 & 0 \\ 0 & 1 & 0 \\ 0 & 0 & 1 \end{bmatrix}\begin{bmatrix} 1 & 0 & 0 \\ 0 & 1 & 0 \\ 0 & \Delta\gamma_1 & 1 \end{bmatrix}\cdots\begin{bmatrix} 1 & 0 & 0 \\ 0 & 1 & 0 \\ 0 & \Delta\gamma_N & 1 \end{bmatrix}$$
$$= \begin{bmatrix} 1 & 0 & 0 \\ 0 & 1 & 0 \\ 0 & \sum_{i=0}^{N}\Delta\gamma_i & 1 \end{bmatrix} = \begin{bmatrix} 1 & 0 & 0 \\ 0 & 1 & 0 \\ 0 & \gamma & 1 \end{bmatrix}. \tag{9}$$

According to Eqs. (7)–(9), we can get

$$\mathbf{F}^{\mathrm{T}} = \mathbf{F}_N^{\mathrm{T}} = \mathbf{F}_{N-1}^{\mathrm{T}}\cdot\mathbf{F}^{\mathrm{T}}(\Delta\gamma_N) = \mathbf{F}_{N-2}^{\mathrm{T}}\cdot\mathbf{F}^{\mathrm{T}}(\Delta\gamma_{N-1})\cdot\mathbf{F}^{\mathrm{T}}(\Delta\gamma_N)$$
$$= \ldots = \mathbf{F}^{\mathrm{T}}(\Delta\gamma_0)\cdot\mathbf{F}^{\mathrm{T}}(\Delta\gamma_1)\cdot\mathbf{F}^{\mathrm{T}}(\Delta\gamma_2)\cdots\mathbf{F}^{\mathrm{T}}(\Delta\gamma_{N-1})\cdot\mathbf{F}^{\mathrm{T}}(\Delta\gamma_N), \tag{10}$$

in which $\mathbf{F}^{\mathrm{T}}$, $\mathbf{F}_n^{\mathrm{T}}$, and $\mathbf{F}^{\mathrm{T}}(\Delta\gamma_n)$ are the transposes of $\mathbf{F}$, $\mathbf{F}_n$, and $\mathbf{F}(\Delta\gamma_n)$, $n = 0, 1, 2, \ldots, N$, respectively. More specifically, in our incremental loading approach, we use the transpose of Eq. (3) in the preceding Comment [2], i.e.,

$$\mathbf{F}_n^{\mathrm{T}} = \mathbf{F}_{n-1}^{\mathrm{T}}\cdot\mathbf{F}^{\mathrm{T}}(\Delta\gamma_n) = \begin{bmatrix} 1 & 0 & 0 \\ 0 & 1 & 0 \\ 0 & \sum_{i=0}^{n-1}\Delta\gamma_i & 1 \end{bmatrix}\begin{bmatrix} 1 & 0 & 0 \\ 0 & 1 & 0 \\ 0 & \Delta\gamma_n & 1 \end{bmatrix},$$

in the nth ($n = 1, 2, \ldots, N$) increment, where $\mathbf{F}_n^{\mathrm{T}}$, $\mathbf{F}_{n-1}^{\mathrm{T}}$, and $\mathbf{F}^{\mathrm{T}}(\Delta\gamma_n)$ correspond to $\mathbf{R}^{\mathrm{def}}$, $\mathbf{R}^{\mathrm{ini}}$, and $\mathbf{F}^{\mathrm{T}}$, respectively. In our original work $\mathbf{F}^{\mathrm{T}}$ is $\mathbf{F}^{\mathrm{T}}(\Delta\varepsilon_{zy}) = \left[\mathbf{I} + \begin{pmatrix} 0 & 0 & 0 \\ 0 & 0 & 0 \\ 0 & \Delta\varepsilon_{zy} & 0 \end{pmatrix}\right]$.

In other cases, such as pure shear and semiconstrained shear, the same incremental loading approach was adopted, but the difference lies in the relaxation mode after each increment of displacement. Furthermore, since the research in Ref. [1] is mainly based on first-principles calculation, to facilitate the reproduction of our work and enable direct production of the POSCAR file, we presented Eq. (10) in our original article, which enabled our writing style to be consistent with that of the renowned literature in this field [5–7]. Moreover, since the relevant method using first-principles calculation is relatively mature, the above derivation process was not presented in our original article.

Therefore, there is no problem using right multiplication in the expression when Eq. (10) is used. As said by Mázdziarz, "it may be worthwhile to use well-established approaches, especially as they come from such giants of intellect like Cauchy and Born." Here we would like to note that the use of left or right multiplications cannot simply rely on rote memorization, but should be applied according to the actual situation.

The strain used in our article [1] is not the Green-Lagrangian strain. It is known that the Green-Lagrangian strain is calculated by $\mathbf{F}$. However, in our work, after each incremental displacement is applied, for simple shear, the size and shape of the supercell remain unchanged, while the coordinates of the internal atoms are optimized; for pure shear, the atomic coordinates and the other five independent components of strain (except ε_{zy}) are optimized simultaneously to reach the pure shear stress state. It is not controlled easily and directly if Green-Lagrangian strain and/or the corresponding stress are used in calculations because they are not defined in the current configuration but in the initial configuration. However, it can be proved that the material

objective of the Green-Lagrangian strain obtained by our method is identical to that obtained from the Green-Lagrangian strain given in the preceding Comment by Mázdziarz [2].

For simple shear, we implemented the deformations through $\dot{\mathbf{F}}$, which, as well as the corresponding results, can be obtained as

$$\mathbf{F}=\begin{bmatrix}1&0&0\\0&1&\gamma\\0&0&1\end{bmatrix},\quad \dot{\mathbf{F}}=\begin{bmatrix}0&0&0\\0&0&\dot{\gamma}\\0&0&0\end{bmatrix},\quad \mathbf{L}=\dot{\mathbf{F}}\cdot\mathbf{F}^{-1}=\begin{bmatrix}0&0&0\\0&0&\dot{\gamma}\\0&0&0\end{bmatrix}\begin{bmatrix}1&0&0\\0&1&-\gamma\\0&0&1\end{bmatrix}=\begin{bmatrix}0&0&0\\0&0&\dot{\gamma}\\0&0&0\end{bmatrix}, \tag{11}$$

$$\boldsymbol{V}=\frac{1}{2}(\mathbf{L}+\mathbf{L}^{\mathrm{T}})=\begin{bmatrix}0&0&0\\0&0&\frac{\dot{\gamma}}{2}\\0&\frac{\dot{\gamma}}{2}&0\end{bmatrix},\quad \mathbf{W}=\frac{1}{2}(\mathbf{L}-\mathbf{L}^{\mathrm{T}})=\begin{bmatrix}0&0&0\\0&0&\frac{\dot{\gamma}}{2}\\0&-\frac{\dot{\gamma}}{2}&0\end{bmatrix}, \tag{12}$$

$$\dot{\mathbf{E}}=\mathbf{F}^{\mathrm{T}}\cdot\boldsymbol{V}\cdot\mathbf{F}=\frac{1}{2}\begin{bmatrix}1&0&0\\0&1&0\\0&\gamma&1\end{bmatrix}\begin{bmatrix}0&0&0\\0&0&\dot{\gamma}\\0&\dot{\gamma}&0\end{bmatrix}\begin{bmatrix}1&0&0\\0&1&\gamma\\0&0&1\end{bmatrix}=\frac{1}{2}\begin{bmatrix}0&0&0\\0&0&\dot{\gamma}\\0&\dot{\gamma}&2\gamma\dot{\gamma}\end{bmatrix}, \tag{13}$$

where $\mathbf{F}$, $\mathbf{L}$, $\boldsymbol{V}$, and $\mathbf{W}$ are the deformation gradient, velocity gradient, rate of deformation, and spin tensor, respectively. Equation (13) is just the material derivative of $\mathbf{E}$ given by Mázdziarz [the material derivative of $\mathbf{E}^{\mathrm{SS}}$ in Eq. (6)].

For pure shear, we did use the pure shear stress state rather than the pure shear deformation mentioned by Mázdziarz, which can be evidenced by Fig. 1(b) and its corresponding description in our original article. The specific approach is that we preset an incremental shear deformation using the same method, but in each step of deformation, the size and shape of the supercell, as well as atomic coordinates, are fully relaxed to reach a pure shear stress state. The reason for adopting this approach is that it is still challenging to perform stress loading in first-principles calculations using VASP. Mázdziarz kindly derived the deformation gradient from a pure shear stress state [Eq. (8)]; unfortunately, it seems that this derivation is based on isotropic constitutive relations, which may not be applicable to the anisotropic supercells of our work. Due to the anisotropy of the supercell and additional anisotropy associated with the relative motion between atoms during deformation in our work, after optimization, some of the supercells may align with the results from Eq. (8) by Mázdziarz and Fig. 2 in our article [1], while others might exhibit tilting in different directions (as shown in Fig. 3 [1]). From the perspective of theoretical analysis, it would require a more rigorous derivation using anisotropic constitutive relationships. For example, if it is anisotropic, Eq. (8) by Mázdziarz may need to be further refined. It would be interesting, but it is not the focus of our work.

The simple shear and pure shear methods using the first-principles calculation align with those in the well-established literature [8–11]. Moreover, our results align with Mázdziarz's, as shown in Figs. 2–4 below. Considering what is mentioned above, our method is reasonable.

Frenkel's sinusoidal solution is actually a reflection of the periodic variation of atomic structure during deformation. It is a simplified model that assumes a perfect crystal lattice without any defects, phase transition, and perturbations during deformation, i.e., $\mathbf{F}$ of any local and global regions remains the same and unchanged during deformation. However, in practice, it is difficult to satisfy all the conditions required for Frenkel's sinusoidal solution. In fact, perturbations and various defects are always present and/or nucleated in materials during deformation, especially at the atomic scale. When performing atomistic simulations, such as first-principles calculations or molecular dynamics simulations, it is important

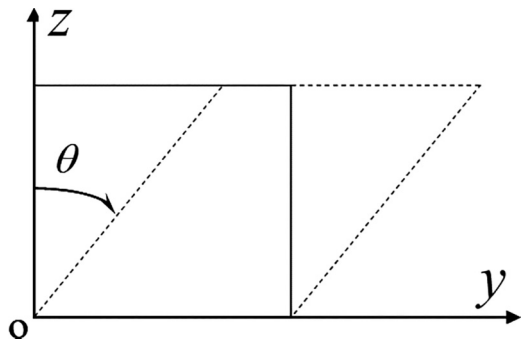

FIG. 1. Schematic of simple shear.

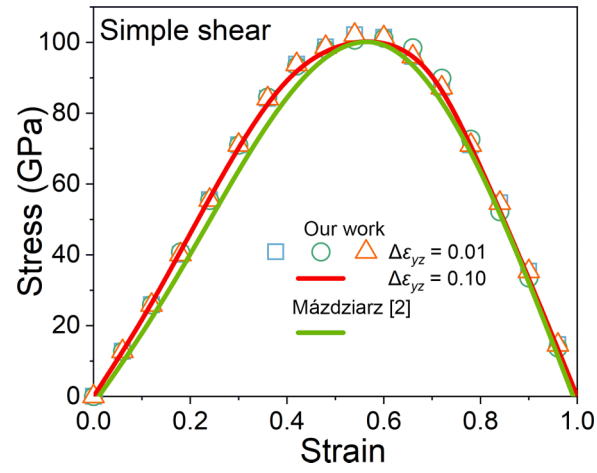

FIG. 2. Stress-strain curves of HfC in the $[1\bar{1}0](110)$ direction calculated by first-principles calculations with the atomic coordinates, size, and shape of the supercell unchanged. Three different parameter settings with strain increments of 0.01 and one stress-strain curve with strain increments of 0.10 are shown, as well as a comparison with the work of Mázdziarz [2].

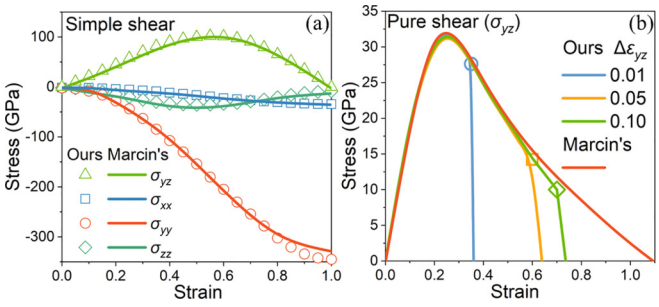

FIG. 3. Stress-strain relations calculated using higher computational accuracy and comparison with that by Mázdziarz [2]. (a) Variations of stress components with ε_{yz} under simple shear with strain increments of 0.01. (b) Variations of σ_{yz} with ε_{yz} under pure shear with strain increments of 0.01, 0.05, and 0.10.

to consider these defects and perturbations in the model. In our work, while the supercells were defect-free single crystals, perturbations were present during relaxation due to the allowance for the optimization of atomic coordinates. We speculated that when the above conditions (perfect crystal lattice without any defects, phase transition, and perturbations during deformation) were strictly satisfied, Frenkel's sinusoidal solution could easily be obtained.

To verify this hypothesis, we perform additional shear deformation using first-principles calculations with specific constraints that keep the atomic coordinates, size, and shape of a supercell unchanged during relaxation after each incremental displacement is applied. Specifically, four sets of simple shear deformation of HfC in the $[1\bar{1}0](110)$ direction ($\Delta\varepsilon_{yz} = 0.01$ with three different parameter settings and $\Delta\varepsilon_{yz} = 0.10$ with one parameter setting) are performed. All stress-strain curves obtained are aligned with Frenkel's sinusoidal solution and close to that presented by Mázdziarz, as shown in Fig. 2 (employing a uniform strain measure). The results also show that the morphology of the stress-strain curve is independent of the strain increment under such conditions.

Although the above results match very well, we consider that they are not meaningful because, in actual deformations, it is impossible to guarantee that the atomic coordinates have no local optimizations, especially at the atomic scale. In addition, it would not be possible to explore various deformation modes without allowing for local atomic coordinate optimization, if we follow Frenkel's solution. However, deformation

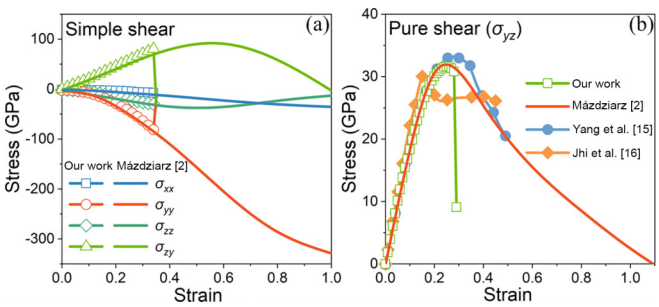

FIG. 4. (a) Comparison of results obtained under simple shear in our article [1] with that by Mázdziarz [2]. (b) Comparison of results obtained under pure shear by us with those by Yang *et al.* [15], Jhi *et al.* [16], and Mázdziarz [2].

mode is one of the focuses of the original article. Therefore, in our article [1], the atomic coordinates are allowed to be optimized, even though we employ the concept of simple shear. It is essential to consider that atoms undergo vibrations around their equilibrium positions rather than remaining fixed in actual deformations.

When allowing the optimization of atomic coordinates, the computed results are dependent on the computational accuracy. We calculated the stress-strain curves of HfC in the $[1\bar{1}0](110)$ direction using higher computational accuracy (the plane-wave cutoff energy is set to 600 eV, and the electronic energy and the ionic force convergence criteria are 10^{-5} eV per supercell and 0.01 eV/Å), as shown in Fig. 3. Figure 3(a) shows the variations of stress components under simple shear, where the stress-strain curve shows sinusoidlike characteristics, which are aligned with that by Mázdziarz (employing a uniform strain measure). Furthermore, it should be noted that the strain increment may significantly affect the stress-strain curve under pure shear, as shown in Fig. 3(b), where there is still a difference in the morphology of the stress-strain curve. Because the deformation is based on the previous step, and the size and shape of the supercell are allowed to change during deformation under pure shear, the stress-strain curve is more affected by the incremental strain step. We utilized three different strain increments to calculate the stress-strain curves, and the stress-strain curve under $\Delta\varepsilon_{yz} = 0.10$ is closest to that presented by Mázdziarz than to others.

As pointed out by a Referee of our original article [1], due to the high symmetry of the cell and the idealized environmental conditions, the point corresponding to the highest stress obtained through first-principles calculations may not accurately represent actual behavior. It is necessary to consider the effects of elastic instability and phonon instability [12], and phonon instabilities may precede the elastic instability for certain states of strain and therefore limit the ideal strength of the material [13,14]. Thus, the significance of obtaining the maximum stress without considering elastic instability and phonon instability is minor.

We compared the results by Mázdziarz with that in our article [1], employing a uniform strain measure, as shown in Fig. 4. It can be seen that our results align precisely with those presented by Mázdziarz, except the primary discrepancy observed at the yield point. Our stress-strain curves only display the yield of the supercell prior to the stress-strain curves indicated by Mázdziarz [Fig. 4(a)]. Because the atomic coordinates are allowed to be optimized, the results in our article [1] differ from those of Mázdziarz and do not always follow Frenkel's sinusoidal solution. In addition, we also extracted the results by Yang *et al.* [15] for comparative analysis [Fig. 4(b)]. It is evident that the values before yield point are identical, and the discrepancy in values can be attributed to the variations in computational accuracy. Different parameter settings and computational accuracy, such as k points and cutoff energy, can lead to divergent yield points. We assume that the variations in k points and energy cutoff can be interpreted as different degrees of perturbation, resulting in deviations in the calculated results.

Introducing displacement perturbations is an approach to consider the influence of elastic instability and phonon

instability [16]. We highlight the need to consider the effects of perturbation, as illustrated in Fig. 5 in our article [1], or to determine stability through phonon calculations. Furthermore, given the complex nature of perturbation effects, we provide an outlook in our article [1], stating the following: "In this work, we use a series of perturbations for shear simulation, but determine the most appropriate perturbation amplitude corresponding to an unstable phonon mode requires further investigation."

Moreover, we extracted the results by Jhi *et al.* [16], as shown in Fig. 4(b), where slight perturbation was introduced into the lattice in each incremental loading, so the lowest critical strain and yield stress were obtained compared with those of the other three stress-strain curves. However, the four stress-strain curves are close to each other reasonably before yield. As was stated in our article [1], "… Fig. 6 shows that the stress-strain curves before yield are also close to each other, indicating that displacement perturbation has little effect on the deformation before yield. … The perturbation mainly affects the yield point, thereby affecting the deformation mode, and the influence before yield can be ignored."

The stress-strain curve obtained through analytical solutions is of significance, but we cannot deny that it is under conditions that are too ideal and difficult to consider the nonuniformity of **F** in actual situations (such as nucleation and motion of dislocations). First-principles calculations can offer a more realistic representation of strength and deformation mode by employing displacement perturbation methods and coupled phonon calculations.

To conclude, some of our work might have been misunderstood. The right multiplication is correct, because we are using the transposed form of **F**. Since we employ first-principles calculations to obtain the mechanical response directly, it is not necessary to consider the finite deformation theory, unless some kind of strain other than $\gamma = \tan\theta$ has to be calculated. Frenkel's sinusoidal solution is an ideal analytical solution that cannot take into account the formation of defects, phase transitions, and the influence of displacement perturbations, which are precisely the progress and advantages of atomic-scale calculations. Therefore, all the results presented are correct and objective.

This work was supported by the National Natural Science Foundation of China (Grants No. 11932004, No. 12272066, and No. 12302130) and Chongqing Natural Science Foundation (Grants No. CSTB2022NSCQ-MSX0383, No. CSTB2022NSCQ-BHX0704, and No. cstc2021jcyj-bshX0240).

[1] C. Li, T. Fu, X. Li, H. Hu, and X. Peng, Phys. Rev. B **107**, 224106 (2023).
[2] M. Mázdziarz, Phys. Rev. B **108**, 216101 (2023).
[3] Z. Zhou, H. Wang, and M. Li, Phys. Rev. B **100**, 024109 (2019).
[4] H. Wang and M. Li, Phys. Rev. Lett. **111**, 065507 (2013).
[5] R. F. Zhang, S. H. Zhang, Y. Q. Guo, Z. H. Fu, D. Legut, T. C. Germann, and S. Veprek, Phys. Rep. **826**, 1 (2019).
[6] S. H. Zhang, Z. H. Fu, and R. F. Zhang, Comput. Phys. Commun. **238**, 244 (2019).
[7] V. Wang, N. Xu, J.-C. Liu, G. Tang, and W.-T. Geng, Comput. Phys. Commun. **267**, 108033 (2021).
[8] S. Ogata, J. Li, and S. Yip, Science **298**, 807 (2002).
[9] M. Jahnátek, J. Hafner, and M. Krajčí, Phys. Rev. B **79**, 224103 (2009).
[10] I. Lobzenko, Y. Shiihara, T. Iwashita, and T. Egami, Phys. Rev. Lett. **124**, 085503 (2020).
[11] C. Liu, X. Song, Q. Li, Y. Ma, and C. Chen, Phys. Rev. Lett. **123**, 195504 (2019).
[12] C. A. Marianetti and H. G. Yevick, Phys. Rev. Lett. **105**, 245502 (2010).
[13] S. M.-M. Dubois, G.-M. Rignanese, T. Pardoen, and J.-C. Charlier, Phys. Rev. B **74**, 235203 (2006).
[14] D. M. Clatterbuck, C. R. Krenn, M. L. Cohen, and J. W. Morris, Jr., Phys. Rev. Lett. **91**, 135501 (2003).
[15] B. Yang, X. Peng, H. Xiang, D. Yin, C. Huang, S. Sun, and T. Fu, J. Alloys Compd. **739**, 431 (2018).
[16] S.-H. Jhi, S. G. Louie, M. L. Cohen, and J. W. Morris, Phys. Rev. Lett. **87**, 075503 (2001).